Infrared Physics & Technology 127 (2022) 104439

Contents lists available at ScienceDirect

Infrared Physics and Technology

journal homepage: www.elsevier.com/locate/infrared

Mid-Infrared spectroscopic characterization: New insights on bioactive molecules of *Olea europaea* L. leaves from selected Italian cultivars

Maria Chiara Di Meo [a,1], Francesco Izzo [b,1], Mariapina Rocco [a], Armando Zarrelli [c], Mariano Mercurio [a], Ettore Varricchio [a,*]

[a] Department of Science and Technology, University of Sannio, Via F. De Sanctis, 82100 Benevento, Italy
[b] Department of Earth Sciences, Environment and Resources, University of Naples Federico II, Via Cintia 21, 80126 Napoli, Italy
[c] Department of Chemical Sciences, University of Naples Federico II, Via Cintia 4, 80126 Napoli, Italy

ARTICLE INFO

Keywords:
Olive leaf (*Olea europaea* L.)
FTIR spectroscopy
Oleuropein
Hydroxytyrosol
PCA analysis
Bioactive molecules

ABSTRACT

Oleuropein and hydroxytyrosol, bioactive molecules present in olive leaves, are well known to have strong beneficial properties for human and animal welfare. Infrared spectroscopy combined to Principal Component Analysis was employed to determine, characterize at molecular level and classify olive leaf from five Italian cultivars (*Caiazzana, Coratina, Ortice, Frantoio, Leccino*) in the different portions (adaxial, abaxial, bulk). The aim of this study was to determine the spectral characteristics, by means of mid-infrared spectroscopy as a rapid tool, in the different portions of the olive leaves to better understand the distribution of the bioactive molecules and to compare the absorption spectra. The results obtained showed that the absorption spectra of the abaxial and adaxial surface of the leaves not only better detect the presence of biomolecules but also present higher levels of oleuropein and hydroxytyrosol for all cultivars analyzed. Therefore, the methods used are potentially useful for discriminating between the different cultivars, the different portions and the bioactive molecules present.

1. Introduction

Olive culture has a great economic and social importance in the Mediterranean area. In addition to oil and olives as main products, the olive-oil supply chain generates large quantities of by-products such as raw olive cake, olive mill wastewater (OMW), twigs and leaves rich in bioactive compounds for food additives, dietary supplements, cosmetic and nutraceutical purpose [1].

Olive leaves are considered to be an economic raw material that can be used as a useful source of high value-added products rich in bioactive substances such as phenolic compounds, triterpenic acids and sugars [2]. The phenolic compounds mainly present in the leaves are oleuropein and hydroxytyrosol [3–5].

Several studies demonstrated the great potential of olive by-product extracts as antioxidants for the food industry and proved that olive leaf extracts (OLEs) are excellent antioxidants with several properties [6]. Nowadays, a large spectrum of beneficial health properties *in vitro* and *in vivo* have been attributed to olive leaves and their extracts, including an important antioxidant effect, anti-hypertensive activity, antimicrobial activity and hypoglycemic effect [7,8]. One of the roles of oleuropein is also to influence the development processes of the olive tree, including defending it against pathogens [9,10].

Additionally, as natural products there are differences in the composition of OLEs due mainly to geographical location, cultivar and plant nutrition so these parameters strongly influence the leaf molecular composition [11].

In this context, the characterization and evaluation of the chemical composition of these products plays an important role in the study of the bioactive molecules present.

Qualitative-quantitative analysis of bioactive molecules in plant matrices (olive leaves) is usually performed using high-performance liquid chromatography (HPLC) [12–15].

However, this analytical method is very expensive and requires long lead times and significant manual work. Associated with this is a complex chemical pre-treatment of the sample and the use of sophisticated analytical instruments [9].

Abbreviations: PCA, principal component analysis; FTIR, Fourier transform infrared; ATR, Attenuated total reflection.

* Corresponding author.
E-mail addresses: mardimeo@unisannio.it (M. Chiara Di Meo), francesco.izzo4@unina.it (F. Izzo), rocco@unisannio.it (M. Rocco), zarrelli@unina.it (A. Zarrelli), mamercur@unisannio.it (M. Mercurio), varricchio@unisannio.it (E. Varricchio).

[1] The authors contributed equally to this work.

https://doi.org/10.1016/j.infrared.2022.104439
Received 31 July 2022; Accepted 27 October 2022
Available online 1 November 2022

Nowadays, the characterization of phenolic compounds using chromatographic techniques (conventional methods) can be overcome by using Fourier Transform Infrared spectroscopy (FTIR) associated with chemometric data analysis (i.e., PCA analysis, cluster analysis) for the determination, characterization, and grouping of the variables (geographical origin, olive cultivars, quality parameters of olives and virgin olive oils, etc.) also determined based on similarities between samples [1,16]. Specifically, the use of advance spectroscopic techniques also allows information to be obtained at the molecular level to characterize olive leaves better [17].

In fact, infrared spectroscopy is among the most widely used techniques for determining molecular structures and identifying compounds in organic and inorganic samples [18–20]. The absorbed energy of infrared radiation results in strain vibrations of specific molecular bonds, e.g. C—H, O—H, N—H, C═O, etc., that are characteristic for the chemical composition of a specific sample [21]. Therefore, FTIR spectra of plant tissues represent a fingerprint of key organic constituents, such as carbohydrates, proteins, lipids, lignins, and other aromatic or other abundant compounds [18].

Actually, FTIR is a simple, fast, and inexpensive instrumental technique used successfully for different types of investigations such as archaeometry and conservation sciences [20,22–24], pharmaceutical [25–27] and biomedical applications [28], environmental issues (e.g. identification of contaminants of emerging concern and threat) [29,30] and fibrous and toxic minerals [31,32].

As far as food applications is concerned FTIR is also used to determine differences in chemical composition between different plant species, but still few studies characterize olive leaves spectroscopically in the different portions (adaxial, abaxial and bulk). The use of Attenuated Total Reflection (ATR) FTIR spectroscopy, which does not require further sample pre-treatment, is presented as a high-throughput method [18]. However, FTIR spectra may likely contain minor differences between two components that could not be distinguished visually, therefore, multivariate data tools such as principal component analysis (PCA) are necessary for spectra analysis. In fact, PCA is an effective variable reduction technique for spectroscopic data in which similar samples appear as clusters in the plot, while different samples appear segregated from each other [33]. It is a non-parametric method for data reduction and provides information about the principal components of spectra that are dominant factors that determine the differences between samples [28]. Several hundred data points (or variants) are found in a typical spectrum, but these variants will usually be correlated with each other to some degree [18]. This method removes the redundancy of having many correlated varying points by transforming the original data into a set of new uncorrelated variants, called principal components (PCs) [34–36]. The resulting plot can reveal clustering or structure in the data set [37] and generate information about the principal components responsible for variability in particular spectrum regions [38].

Due to a lack of scientific data on the spectroscopic characterization, by means of ATR-FTIR technology, in the different portions (adaxial - upper, abaxial – lower and bulk) of olive leaves in the five Italian cultivars analyzed (*Caiazzana, Coratina, Ortice, Frantoio* and *Leccino*), in this study we wanted to characterize this type of plant matrix spectroscopically also on the basis of the presence and distribution of bioactive molecules (oleuropein and hydroxytyrosol) in olive leaves.

The study of surface areas of leaves is essential because these surfaces are strongly influenced by wax thickness and trichomes abundance, factors that can determine spectral differences between adaxial and abaxial leaf surfaces [39]. Phenolic compounds are also among the main components expressed in leaf surface portions and diffused in the upper portion of the plant cuticle between the epicuticular wax layer and the lower polysaccharide-rich portion [40].

Actually, the aim of the present study is to determine the spectral characteristics of the leaves in the different portions using the ATR-FTIR spectroscopy method, associating this method with multivariate statistical analysis to better understand the distribution of the bioactive molecules and compare the spectra between different olive cultivars in leaf portions.

2. Materials and methods

2.1. Leaf samples

Olive leaves belonging to five different cultivars (namely *Caiazzana*, *Coratina*, *Ortice*, *Frantoio* and *Leccino*), growing under the same agronomic conditions, were collected on March from the Middle Valley of Volturno River (Ruviano, Southern Italy) at about 110 m above sea level. According to Di Meo et al. [5], olive leaves were harvested during the phenological phase (March) with the highest concentration of bioactive molecules and high antioxidant activity for the cultivars here analyzed. This period corresponds to pruning of olive leaves and the vegetative recovery phase. Leaves were collected from several trees and from different parts of each tree, in order to minimize the effect of sun exposure and differences related to different developmental stages [5].

Different leaf portions were here spectroscopically analyzed: adaxial - top surface, abaxial - bottom surface and the whole (bulk) shredded leaf. According to Di Meo et al. [5] the shredded bulk leaf was characterized by HPLC-UV analysis in order to determine concentration of bioactive molecules; a high content of oleuropein and hydroxytyrosol was found in the leaves of the Caiazzana cultivar harvested in March compared to the other cultivars analyzed (oleuropein: 72.08 ± 1.23 mg/g of dry extract and hydroxytyrosol: 0.43 ± 0.06 mg/g of dry extract). Collected leaves were air dried at room temperature (20 °C) for 10 days as they maintained a constant weight from the seventh day. For adaxial and abaxial surface analysis the dried leaves were analyzed as they are, while the bulk dried leaves were crushed with a blade mixer to obtain a powder filtered through a standard 125 μm sieve. The sieved powder was collected and stored at room temperature in the dark in airtight bags until use.

The characterization of the bioactive molecules present in the olive leaves of the five different cultivars was carried out by HPLC and showed the two phenolic compounds most present in the leaves, such as oleuropein and hydroxytyrosol, present in different quantities: statistically higher values of oleuropein than hydroxytyrosol in the five cultivars analyzed. The cultivars that presented higher levels of bioactive molecules than the other ones analyzed were *Caiazzana* and *Coratina*.

2.2. FTIR spectroscopy

To obtain information about the functional group compositions of the main components of the leaf surface (both adaxial and abaxial sides) and crushed bulk samples, olive leaves have been characterized in Fourier Transform Infrared spectroscopy by means of a Bruker Alpha spectrometer in Attenuated Total Reflectance (FTIR-ATR) mode (spectral range 4000–400 cm^{-1}, resolution 4 cm^{-1}, 128 scans). The spectra were processed using the software Opus 7.8 (Bruker, Optics GmbH). Particularly, after averaging of 5 different measurements, each FTIR spectrum underwent to baseline correction, smoothing, second derivative and peak picking. FTIR measurements were also carried out, at same experimental conditions, on the bioactive molecules oleuropein (CAS No.32619–42-4, Sigma-Aldrich St. Louis, MO, USA) and hydroxytyrosol (CAS No.10597–60-1, Sigma-Aldrich St. Louis, MO, USA).

2.3. Principal components analysis (PCA)

To achieve a more accurate indication of the results obtained, we performed a PCA by selecting a specific spectral region (1800–950 cm^{-1}) representative of the absorption bands of the phenolic compounds downstream of the spectroscopic characterization.

PCA was performed to better understand the relationships between spectroscopical features of leaf and analyzed biomolecules, as well as to highlight main differences between the five selected cultivars.

In fact, in our study to identify similarities or differences between olive leaf samples of the five cultivars and the distribution of bioactive molecules in the different leaf portions (bulk, adaxial and abaxial), the ClustVis (**https://biit.cs.ut.ee/clustvis/**) online program package was employed [41]. During model development, IR spectra and reference values for oleuropein and hydroxytyrosol and the different portions of the five cultivars studied were used.

3. Results and discussion

3.1. FTIR

A representative FTIR spectrum of crushed bulk *Olea europaea* leaf (i.e., *Caiazzana* cultivar) is shown in Fig. 1a, whereas its second derivative is reported in Fig. 1b. On the other hand, Fig. 1c, d display the mid-infrared spectra of adaxial and abaxial leaf surfaces, respectively for the same cultivar. FTIR spectra of oleuropein and hydroxytyrosol were also reported in Fig. 1e, f.

As a whole, FTIR spectra of crushed bulk samples are very consistent to other spectral patterns reported in literature for the same plant species [9,15,42].

Particularly, FTIR spectra of examined leaf samples are characterized by similar absorption bands as demonstrate by their positions and relative intensities of the main absorption bands summarized in Table 1, along with a tentative assignment vibration. This matter may make it difficult to discriminate the selected cultivars only by visual examination, although some weak differences can be observed in terms of relative intensities of absorbance. Usually, a second derivative treatment of spectra (Fig. 1b) could highlight the occurrence of some hidden signals (generally consisting in shoulders) and allow a correct peak-picking of them.

In spite their complex chemical composition, some general considerations about the spectral features of olive leaves can be carried out. Firstly, all spectra show the occurrence in the higher wavenumber region (4000–1800 cm^{-1}) of a broad absorption band centered at around 3280 cm^{-1} in bulk samples and at around 3380 cm^{-1} in uncrushed ones. The same band also appears in FTIR spectrum of oleuropein (3339 cm^{-1}). This band is often observed both in organic and inorganic materials [20,43] and can be generally attributable to the stretching vibration of hydroxyl groups in the O—H bond. This band in leaves could

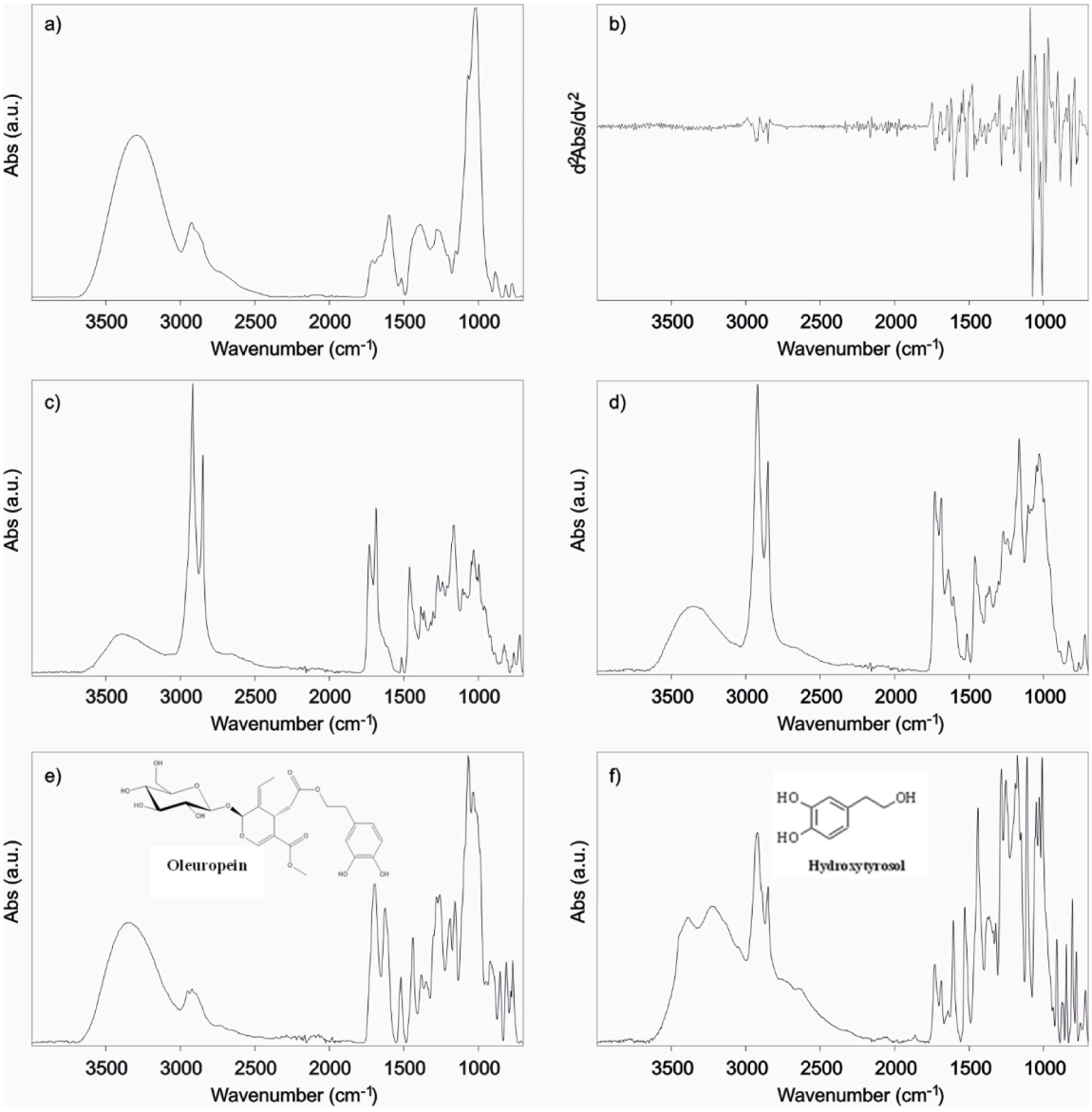

Fig. 1. Representative FTIR spectra of *O. europaea* leaf sample (*Caiazzana* cultivar): a) FTIR spectrum of crushed bulk sample and b) its second derivative; c) and d) FTIR spectra of leaf surfaces (respectively adaxial and abaxial sides); e) FTIR spectrum of oleuropein; f) FTIR spectrum of hydroxytyrosol.

Table 1
Main absorption bands (expressed in cm^{-1}) observed for the examined *O. europaea* L. leaves and bioactive molecules. Legend: ν, stretching; δ, bending; γ, out-of-plane bending; a, asymmetric; s, symmetric; br, broad; w, weak; vw, very weak; m, medium; s, strong; vs very strong; sh, shoulder.

Tentative assignment vibration	Caiazzana bulk	Coratina bulk	Frantoio bulk	Leccino bulk	Ortice bulk	Caiazzana adaxial	Coratina adaxial	Frantoio adaxial	Leccino adaxial	Ortice adaxial	Caiazzana abaxial	Coratina abaxial	Frantoio abaxial	Leccino abaxial	Ortice abaxial	Oleuropein	Hydroxytyrosol
ν(O—H)	–	–	–	–	–	–	–	–	–	–	–	–	–	–	–	–	3387 br
ν(O—H)	3290 br	3277 br	3284 br	3269 br	3266 br	3391 br	3399 br	3393 br	3401 br	3398 br	3359 br	3377 br	3361 br	3364 br	3380 br	3339 br	–
ν(O—H)	–	–	–	–	–	–	–	–	–	–	–	–	–	–	–	–	3225 br
ν_a(C—H) alkyl	–	–	–	–	–	–	–	–	–	–	–	–	–	–	–	2951 w	–
ν_a(C—H) alkyl	2926 w	2929 w	2919 w	2932 w	2928 w	2917 vs	297 vs	2917 vs	2917 vs	2917 vs	2919 vs	2918 vs	2919 vs	2919 vs	2919 vs	2922 w	2921 s
ν_s(C—H) alkyl	2849 sh	2850 sh	2850 sh	2850 sh	2850 sh	2849 vs	2849 vs	2849 vs	2849 vs	2849 vs	2850 vs	2850 vs	2850 vs	2850 vs	2850 vs	2850 vs	2850 s
ν(C═O) ester	1709 vw	1709 vw	1710 vw	1710 vw	1733 sh	1732 s	1732 s	1733 s	1730 s	1732 s	1730 s	1730 s	1730 s	1730 s	1730 s	1730 s	1731 m
ν(C═O) acid	–	–	–	–	–	1686 s	1686 s	1686 s	1686 s	1686 s	1687 s	1687 s	1687 s	1687 s	1687 s	1698 s	1687 m
ν(C═C) acid	–	–	–	–	–	–	–	–	1640 sh	–	1639 m	1639 m	1640 m	1639 m	1638 m	1626 s	1641 w
ν(C—C) aromatic	1599 m	1601 m	1597 m	1603 m	1596 m	1606 sh	–	–	1608 sh	–	1605 m	1604 sh	1605 m	1606 sh	1606 sh	–	1608 m
ν(C—C) aromatic	–	–	–	–	–	–	–	–	1549 vw	–	1548 vw	1552 vw	1549 vw	1549 vw	–	–	–
ν(C—C) aromatic	1516 vw	1516 vw	1516 vw	1516 vw	1515 vw	1516 w	1517 w	1515 w	1516 w	1517 w	1514 w	1515 w	1514 w	1514 w	1514 w	1520 m	1529 m
δ(C—H) scissoring	–	–	–	–	–	1462 m	1462 m	1462 m	1462 m	1462 m	1462 m	1462 m	1462 m	1462 m	1462 m	1439 m	1441 s
ν(C—C) aromatic (conjugated with C═C)	–	–	–	–	–	1415 sh	1416 sh	1415 sh	1416 sh	1417 sh	1415 sh	1415 sh	1415 sh	1417 sh	1418 sh	–	–
δ(C—H) wagging and twisting	1386 m	1385 m	1385 m	1377 m	1387 m	1386 m	1386 m	1386 m	1386 m	1386 m	1385 sh	1386 sh	1386 sh	1386 sh	1386 sh	1382 m	1366 m
δ(C—H) wagging and twisting	–	–	–	–	–	1364 m	1364 m	1364 m	1365 m	1364 m	1365 m	1364 m	1365 m	1365 m	1365 m	1350 m	–
δ(C—H)	–	1315 vw	–	1316 vw	1316 vw	1321 vw	1321 vw	1321 vw	1321 vw	1321 vw	1319 vw	1320 vw	1320 vw	1320 vw	1319 vw	1319 vw	1321 m
δ(C—H)	–	–	–	–	–	1303 vw	1304 vw	1303 vw	1303 vw	1304 vw	1303 vw	1303 vw	1303 vw	1303 vw	1303 vw	1301 sh	–
δ(C—H)	1260 m	1259 m	1259 m	1260 m	1260 m	1270 m	1270 m	1269 m	1270 m	1270 m	1269 m	1270 m	1269 m	1269 m	1270 m	1280 m	1284 vs
δ(OH)	–	–	–	–	–	1239 m	1240 m	1240 m	1240 m	1240 m	1239 m	1240 m	1240 m	1240 m	1240 m	1260 m	1253 vs
ν_a(C—O—C)	1203 sh	1204 sh	1202 sh	1199 sh	1199 sh	1211 sh	1211 sh	1211 sh	1210 sh	1211 sh	1211 sh	1211 sh	1211 sh	1210 sh	1211 sh	1190 m	1189 sh/1175 vs
ν_a(C—O—C)	1151 sh	1152 sh	1150 sh	1151 sh	1148 sh	1165 m	1166 m	1165 m	1165 m	1166 m	1164 s	1165 s	1164 s	1164 s	1164 s	1156 m	1151 sh
ν_s(C—O—C)	–	–	–	–	–	1105 m	1105 m	1105 m	1105 m	1105 m	1104 s	1104 s	1104 s	1104 s	1104 s	1095 sh	–
ν_s(C—O—C)	–	–	–	–	–	1092 m	1092 m	1092 m	1092 m	1092 m	1084 s	1082 s	1087 s	1086 s	1083 s	1068 s	1049 vs
ν_s(C—O—C)	1069 vs	1070 vs	1067 vs	1072 vs	1073 vs	1046 sh	1046 sh	1045 sh	1045 sh	1045 sh	1049 vs	1047 vs	1047 vs	1046 vs	1048 vs	1036 s	1028 vs
ν(C—O—C), glycosydic bond	1016 vs	1021 vs	1014 vs	1021 vs	1020 vs	1031 m	1032 m	1031 m	1032 m	1032 m	1029 s	1029 s	1029 s	1029 s	1029 s	1015 s	1009 vs
ν(C—O)	–	–	–	–	–	997 m	997 m	997 m	997 m	997 m	997 sh	998 sh	997 sh	997 sh	998 sh	988 sh	–

(*continued on next page*)

Table 1 (*continued*)

Tentative assignment vibration	Caiazzana	Coratina	Frantoio	Leccino	Ortice	Caiazzana	Coratina	Frantoio	Leccino	Ortice	Caiazzana	Coratina	Frantoio	Leccino	Ortice	Oleuropein	Hydroxytyrosol
	bulk	bulk	bulk	bulk	bulk	adaxial	adaxial	adaxial	adaxial	adaxial	abaxial	abaxial	abaxial	abaxial	abaxial		
ν(C—O)	–	–	–	–	–	959 sh	960 sh	961 sh	960 sh	960 sh	960 sh	951 sh	957 sh	958 sh	957 sh	947 vw	–
γ(C—H)	922 vw	930 vw	927 vw	930 vw	930 vw	918 sh	917 sh	917 sh	917 sh	917 sh	918 sh	918 sh	916 sh	917 sh	918 sh	920 m	911 m
γ(C—H)	885 w	887 w	885 w	888 w	888 w	887 vw	887 vw	887 vw	887 vw	887 vw	888 vw	886 vw	887 vw	888 vw	887 vw	893 sh	876 m
γ(C—H) aromatic	815 vw	814 vw	815 vw	815 vw	815 vw	826 w	826 w	826 w	827 w	826 w	832 w	832 w	833 w	832 w	833 w	854 m	847 m
γ(C—H) aromatic	–	–	–	–	–	–	–	–	–	–	–	–	–	–	–	812 m	807 m
γ(C—H) aromatic	–	–	–	–	–	–	–	–	–	–	–	–	–	–	–	783 sh	781 m
γ(C—H) aromatic	769 vw	771 vw	770 vw	769 vw	765 vw	763 vw	763 vw	763 vw	762 vw	763 vw	764 vw	763 vw	763 vw	763 vw	763 vw	768 m	752 vw
δ(C—H) rocking	–	–	–	–	–	721 w	721 w	721 w	722 w	721 w	723 w	722 w	723 w	722 w	723 w	713 vw	719 w
Esterification Index	0.50 ± 0.01	0.49 ± 0.03	0.38 ± 0.11	0.46 ± 0.03	0.33 ± 0.02	0.45 ± 0.03	0.36 ± 0.01	0.48 ± 0.04	0.48 ± 0.02	0.39 ± 0.04	0.55 ± 0.08	0.71 ± 0.01	0.64 ± 0.02	0.62 ± 0.02	0.75 ± 0.02	–	–

be related to the simultaneous contribution of compounds such as polysaccharides, acids, oleuropein and non-esterified hydroxyl groups of cutin (especially in the examination of cuticles) [40]. In hydroxytyrosol OH groups stretching vibrations are observed at ca. 3387 and 3225 cm^{-1}.

In the spectral range 3000–2800 cm^{-1}, a couple of bands is representative of the asymmetric and symmetric of CH_3 and CH_2 groups in long chain aliphatic compounds and are observed in all examined samples. In the external surface of leaf, these bands are emphasized by the spectral contribution of cutin and epicuticular waxes [44]. It is worthy that the absorption intensities of these bands are almost similar between adaxial and abaxial sides of olive leaves. It could be explained by a similar amount of epicuticular wax onto the two leaf surfaces. This hypothesis accounts with the wax yield values for the dehaired lamina of *O. europaea* leaves available in literature [45].

Most of the mid-infrared spectral features of natural compounds, including those of bulk and surface components of leaves, are gathered in the so-called fingerprint regions [46], namely from 1800 cm^{-1} to 700 cm^{-1}, or over especially in the case of inorganic phases [24,47]. According to the literature [9,42], the absorption bands located between 1800 and 1500 cm^{-1} could be related to the stretching vibrations of C═O and C═C bonds. In fact, the band at around 1715–1730 cm^{-1} is generally attributable to C═O stretching vibration of esters. This band appears definitely strong, in terms of relative intensities, in FTIR spectra of leaf surfaces (Fig. 1 c, d), as a consequence of the spectral contribution of cutin. Furthermore, the relative intensity of this peak seems to be stronger in abaxial surface than in adaxial side, leading to a higher esterification index, namely the ratio between the absorbance intensity of this absorption band with the asymmetric stretching vibration ν(C—H) at ca. 2916 cm^{-1} [48,49]. The difference in the esterification index between the two leaf surfaces could be due also to the occurrence of a higher amount of trichomes in the abaxial leaf surface for *O. europaea* [45]. A strong band at ca. 1730 cm^{-1} also appears in oleuropein, whereas it shows a medium intensity in hydroxytyrosol. Another band, clearly observed in leaf surfaces and bioactive molecules, is located around 1686–1698 cm^{-1} as a consequence of stretching vibrations of C═O bonds in carboxylic acids.

In adaxial and even more in abaxial leaf surfaces, it is possible to observe a sequence of spectral features, with variable intensity (Table 1), generally attributable to the phenolic compounds scattered in the uppermost part of plant cuticles [40]. These bands are mainly located between 1650 and 1400 cm^{-1}. The stretching vibration of C═C of phenolic acids is centered around 1640 cm^{-1} and is also observed in oleuropein (1626 cm^{-1}) and hydroxytyrosol (1641 cm^{-1}) but not in crushed bulk leaves. A common band at around 1600–1608 cm^{-1} is representative of C—C aromatic stretching vibration in all samples, whereas the bands at ca. 1550, 1515, 1460 and 1415 could be related to C—C aromatic stretching vibration conjugated with C═C. Phenolic compounds of cuticle can be observed thanks to the beam penetration depth (d_p) of ATR that generally ranged from 0.5 μm to 5 μm, according to experimental conditions [44,46,48]. Finally, an additional band related to phenolic compounds was detected at lower wavenumber, particularly at ca. 833 cm^{-1} and it is considered representative of the out-of-plane bending vibrations of C—H.

The remaining part of FTIR spectra is composed by complex spectral features mainly consisting in bending vibrations of C—H and O—H functional groups of cutin, waxes and polysaccharides (1500–1200 cm^{-1}), as well as the stretching vibrations of C—O—C bonds in polysaccharides (1150–950 cm^{-1}). The latter reach the highest absorption intensities in bulk leaf samples and lowest ones in the adaxial surfaces (Table 1).

3.2. Principal components analysis

Principal component analysis represents a multivariate method used for data analysis in different fields [1,50,51]. In our study, bioactive

molecules and cultivars were subjected to PCA to identify peculiar relationships, similarities and differences in the analyzed cultivar groups [52].

From the FTIR spectra, using the appropriate software, it was possible to perform a multivariate analysis, performing a PCA with the aim of investigating similarities and/or differences between cultivars, in particular to discriminate the leaf portions and evaluate the oleuropein and hydroxytyrosol distribution in the cultivars.

As revealed by spectroscopic analysis, PCA also showed similar characteristics in the adaxial and abaxial surfaces but with the formation of three different clusters and therefore distinguishable from each other and different from the bulk. This analysis can be used to estimate whether predefined groups form separate or overlapping clusters [41]. PCA results are presented by a biplot (Fig. 2) in order to determine the contribution of bioactive molecules and the distribution of cultivars in the different portions. The first two main components represent 79.4 % and 13 % of the total data variability, respectively. The plot shows three separate clusters for the portions considered and a clear similarity between cultivars in a given portion. In particular, the adaxial and abaxial surfaces are closer and therefore more similar to each other.

Fig. 2 shows that the cultivars are similar to each other but partly distinguishable, the difference is between the portions. The bulk portion is negatively correlated to PC1, while adaxial and a part of abaxial (excluding the *Coratina* cultivar) is positively correlated to PC1. The abaxial portion and part of the adaxial (excluding the *Coratina* and *Ortice* cultivars) are positively correlated to PC2. The bioactive molecules (oleuropein and hydroxytyrosol) are positively correlated to PC1 and negatively correlated to PC2. Biplot shows that oleuropein and hydroxytyrosol are closer to the abaxial and adaxial portions, indicating a greater presence of these bioactive molecules in the lower and upper surface of the olive leaf for all cultivars analyzed. This is a clear indication of what was obtained from the spectroscopic analysis. PCA allowed to extract and visualize the main information from the dataset in order to examine the qualitative differences between the clusters. In this perspective, this study shows that FTIR-ATR spectroscopy with PCA analysis are potentially useful methods for discriminating between different cultivars, portions and bioactive molecules.

4. Conclusions

Due to the importance of olive leaves as a natural source of antioxidants with high polyphenols content, characterization, spectroscopic analysis and PCA analysis to discriminate cultivars and distribution of bioactive molecules are essential. HPLC characterization can be overcome by FTIR-ATR spectroscopic characterization and multivariate statistical analysis (PCA), reducing run times and avoiding sample pretreatment.

Our study shows that FTIR-ATR spectroscopy in combination with PCA is suitable to discriminate different cultivars from different territorial areas but specially to evaluate differences/similarities between the different leaf portions and the distribution of the bioactive molecules.

The present work has made it possible to investigate FTIR spectroscopic characterization of olive leaves, of the whole leaf and the superficial portion (abaxial and adaxial). The spectroscopic analysis of the leaf surfaces makes it possible to reach a sufficient level of detail to investigate the molecular composition of the main functional leaf traits (epicuticular wax, trichomes, polysaccharides, etc.).

This highlights the spectral polyphenols response, which in bulk samples is substantially hidden by the intense absorption bands of the polysaccharide compounds; in fact, the adaxial and abaxial spectra are more defined than in bulk spectrum. There are differences between the lower and upper leaf surfaces mainly related to the presence of trichomes, the epicuticular wax and consequently the esterification index.

It was possible to hypothesize that these biomolecules are better detectable and probably quantifiable by chemometric analysis using the absorption spectrum of the leaf surface instead of its bulk. Therefore, the results allow us to lay the foundations for a new chemometric approach for the identification and quantification of bioactive molecules. It is clearly necessary to deepen and intensify the dataset with a larger number of significant samples to train an automated classification and/or prediction system (machine learning, PLS, neural network, genetic algorithms). It is also not to be excluded that in-depth spectroscopic characterization can be applied in further applications both in the agri-food field and in forensic or environmental applications.

The experimental approach allowed us to identify the presence and distribution of polyphenols in the various portions of the leaf and to highlight differences among different cultivars.

Since polyphenols are secondary plant metabolites that act as a defense against possible external insults, it is possible to identify cultivars that are potentially more resistant to phytopathological attacks. Thus, the application of the spectroscopic technique, coupled with chemometric analysis, represents a rapid assessment to better understand, at different phenological phases, the plant's defense to phytopathologies as a tool to support management decisions for possible reduction of phytosanitary treatments in agriculture.

In addition, the large-scale application of these techniques can be a valuable aid in the extraction processes of phenolic molecules present in plant matrices or by-products of agri-food supply chains to be used from the perspective of the corporate circular economy.

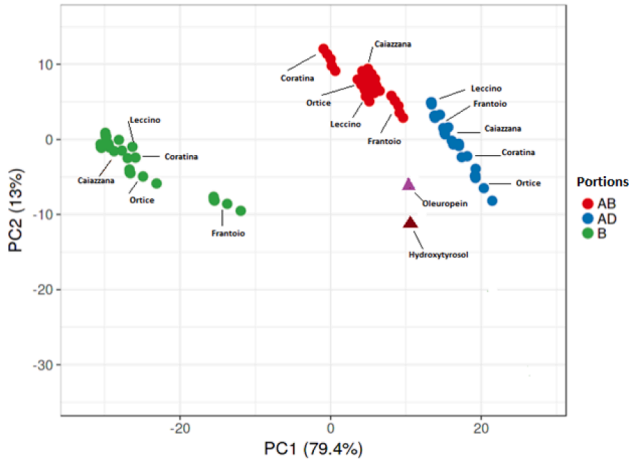

Fig. 2. Biplot of principal component analysis (PCA) of cultivars in different portions and distribution of bioactive molecules (oleruropein and hydroxytyrosol) through ClustVis online program package (https://biit.cs.ut.ee/clustvis/). Portion AB (abaxial), AD (adaxial) and B (bulk).

CRediT authorship contribution statement

Maria Chiara Di Meo: Conceptualization, Formal analysis, Data curation, Investigation, Methodology, Validation, Visualization, Writing – original draft. **Francesco Izzo:** Conceptualization, Formal analysis, Data curation, Investigation, Methodology, Validation, Visualization, Writing – original draft. **Mariapina Rocco:** Visualization, Investigation, Validation. **Armando Zarrelli:** Visualization, Investigation, Data curation, Validation. **Mariano Mercurio:** Visualization, Investigation, Validation, Writing – review & editing. **Ettore Varricchio:** Conceptualization, Visualization, Investigation, Validation, Funding acquisition, Writing – review & editing.

Declaration of Competing Interest

The authors declare that they have no known competing financial interests or personal relationships that could have appeared to influence the work reported in this paper.

Data availability

Data will be made available on request.

Acknowledgements

Thanks to the Taburno Local Action Group (Gal) under Local Development Strategy (Ssl), Measure 16.1 Action 2, supported by PSR Campania 2014-2020 for funding the Rinnoliva project “Productive strategies for the enhancement and renewal of Sannita olive growing” in which this study is included. Scientific Responsible: Prof. Ettore Varricchio.

References

[1] M. De Luca, W. Terouzi, G. Ioele, F. Kzaiber, A. Oussama, F. Oliverio, R. Tauler, G. Ragno, Derivative FTIR spectroscopy for cluster analysis and classification of morocco olive oils, Food Chem. 124 (2011) 1113–1118, https://doi.org/10.1016/j.foodchem.2010.07.010.

[2] E. Medina, C. Romero, P. García, M. Brenes, Characterization of bioactive compounds in commercial olive leaf extracts, and olive leaves and their infusions, Food Funct. 10 (2019) 4716–4724, https://doi.org/10.1016/j.ceramint.2018.12.204.

[3] Á. Guinda, J.M. Castellano, J.M. Santos-Lozano, T. Delgado-Hervás, P. Gutiérrez-Adánez, M. Rada, Determination of major bioactive compounds from olive leaf, LWT-Food Sci. Technol. 64 (2015) 431–438, https://doi.org/10.1016/j.lwt.2015.05.001.

[4] D. Martín-Vertedor, M. Garrido, J.A. Pariente, J. Espino, J. Delgado-Adámez, Bioavailability of Bioactive Molecules from Olive Leaf Extracts and its Functional Value: Potential Health Benefits of Olive Leaf Extract, Phytother. Res. 30 (7) (2016) 1172–1179.

[5] M.C. Di Meo, G.A. De Cristofaro, R. Imperatore, M. Rocco, D. Giaquinto, A. Palladino, T. Zotti, P. Vito, M. Paolucci, E. Varricchio, Microwave-Assisted Extraction of Olive Leaf from Five Italian Cultivars: Effects of Harvest-Time and Extraction Conditions on Phenolic Compounds and In Vitro Antioxidant Properties, ACS Food Sci. Technol. 2 (2021) 31–40, https://doi.org/10.1021/acsfoodscitech.1c00227.

[6] T.M. Keceli, F. Harp, The effect of olive leaves and their harvest time on radical scavenging activity and oxidative stability of refined olive oil, Qual. Assur. Saf. Crop. Foods. 6 (2014) 141–149, https://doi.org/10.3920/QAS2013.0305.

[7] S.N. El, S. Karakaya, Olive tree (Olea europaea) leaves: potential beneficial effects on human health, Nutr. Rev. 67 (2009) 632–638, https://doi.org/10.1111/j.1753-4887.2009.00248.x.

[8] M. Ben Salem, H. Affes, K. Ksouda, Z. Sahnoun, K.M. Zeghal, S. Hammami, Pharmacological Activities of O lea europaea Leaves, J. Food Process. Preserv. 39 (2015) 3128–3136, https://doi.org/10.1111/jfpp.12341.

[9] F. Aouidi, N. Dupuy, J. Artaud, S. Roussos, M. Msallem, I.P. Gaime, M. Hamdi, Rapid quantitative determination of oleuropein in olive leaves (*Olea europaea*) using mid-infrared spectroscopy combined with chemometric analyses, Ind. Crops Prod. 37 (2012) 292–297, https://doi.org/10.1016/j.indcrop.2011.12.024.

[10] N.S.A. Malik, J.M. Bradford, Changes in oleuropein levels during differentiation and development of floral buds in ‘Arbequina’olives, Sci. Hortic. 110 (2006) 274–278, https://doi.org/10.1016/j.scienta.2006.07.016.

[11] A.N. Sudjana, C. D’Orazio, V. Ryan, N. Rasool, J. Ng, N. Islam, T.V. Riley, K. A. Hammer, Antimicrobial activity of commercial *Olea europaea* (olive) leaf extract, Int. J. Antimicrob. Agents. 33 (2009) 461–463, https://doi.org/10.1016/j.ijantimicag.2008.10.026.

[12] C. Savournin, B. Baghdikian, R. Elias, F. Dargouth-Kesraoui, K. Boukef, G. Balansard, Rapid high-performance liquid chromatography analysis for the quantitative determination of oleuropein in *Olea europaea* leaves, J. Agric. Food Chem. 49 (2001) 618–621, https://doi.org/10.1021/jf000596+.

[13] R. Japón-Luján, J.M. Luque-Rodríguez, M.D.L. De Castro, Dynamic ultrasound-assisted extraction of oleuropein and related biophenols from olive leaves, J. Chromatogr. A. 1108 (2006) 76–82, https://doi.org/10.1016/j.chroma.2005.12.106.

[14] A. Ranalli, S. Contento, L. Lucera, M. Di Febo, D. Marchegiani, V., Di Fonzo, Factors affecting the contents of iridoid oleuropein in olive leaves (*Olea europaea* L.), J. Agric. Food Chem. 54 (2006) 434–440, https://doi.org/10.1021/jf051647b.

[15] F. Aouidi, N. Dupuy, J. Artaud, S. Roussos, M. Msallem, I. Perraud-Gaime, M. Hamdi, Discrimination of five Tunisian cultivars by Mid InfraRed spectroscopy combined with chemometric analyses of olive *Olea europaea* leaves, Food Chem. 131 (2012) 360–366, https://doi.org/10.1016/j.foodchem.2011.08.041.

[16] A. Bendini, L. Cerretani, A. Carrasco-Pancorbo, A.M. Gómez-Caravaca, A. Segura-Carretero, A. Fernández-Gutiérrez, G. Lercker, Phenolic molecules in virgin olive oils: a survey of their sensory properties, health effects, antioxidant activity and analytical methods. An overview of the last decade Alessandra, Molecules 12 (2007) 1679–1719, https://doi.org/10.3390/12081679.

[17] M. González-Cabrera, A. Domínguez-Vidal, M.J. Ayora-Cañada, Hyperspectral FTIR imaging of olive fruit for understanding ripening processes, Postharvest Biol. Technol. 145 (2018) 74–82, https://doi.org/10.1016/j.postharvbio.2018.06.008.

[18] R. Rana, G. Müller, A. Naumann, A. Polle, FTIR spectroscopy in combination with principal component analysis or cluster analysis as a tool to distinguish beech (Fagus sylvatica L.) trees grown at different sites, Holzforschung 62 (2008) 530–538, https://doi.org/10.1515/HF.2008.104.

[19] E. Lazzari, T. Schena, M.C.A. Marcelo, C.T. Primaz, A.N. Silva, M.F. Ferrao, T. Bjerk, E.B. Caramao, Classification of biomass through their pyrolytic bio-oil composition using FTIR and PCA analysis, Ind. Crops Prod. 111 (2018) 856–864, https://doi.org/10.1016/j.indcrop.2017.11.005.

[20] F. Izzo, C. Germinario, C. Grifa, A. Langella, M. Mercurio, External reflectance FTIR dataset (4000–400 cm^{-1}) for the identification of relevant mineralogical phases forming Cultural Heritage materials, Infrared Phys. Technol. 106 (2020), 103266, https://doi.org/10.1016/j.infrared.2020.103266.

[21] H. Günzler, H.-U. Gremlich, IR spectroscopy, An introduction (2002).

[22] C. Germinario, G. Cultrone, A. De Bonis, F. Izzo, A. Langella, M. Mercurio, V. Morra, A. Santoriello, S. Siano, C. Grifa, The combined use of spectroscopic techniques for the characterisation of Late Roman common wares from Benevento (Italy), Meas. J. Int. Meas. Confed. 114 (2018) 515–525, https://doi.org/10.1016/j.measurement.2016.08.005.

[23] M. Mercurio, C. Germinario, C. Grifa, F. Izzo, A. Langella, Non-invasive FTIR spectroscopy: New preliminary data for the identification of mineralogical phases forming Cultural Heritage materials, Rend. Online Soc. Geol. Ital. 42 (2017). 115-118- https://doi.org/10.3301/ROL.2017.27.

[24] M. Mercurio, M. Rossi, F. Izzo, P. Cappelletti, C. Germinario, C. Grifa, M. Petrelli, A. Vergara, A. Langella, The characterization of natural gemstones using non-invasive FT-IR spectroscopy: New data on tourmalines, Talanta 178 (2018) 147–159, https://doi.org/10.1016/j.talanta.2017.09.030.

[25] S.R. Matkovic, G.M. Valle, L.E. Briand, Quantitative analysis of ibuprofen pharmaceutical formulations through FTIR spectroscopy, Lat. Am. Appl. Res. 35 (2005) 189–195.

[26] B. de Gennaro, M. Mercurio, P. Cappelletti, L. Catalanotti, A. Daković, A. De Bonis, C. Grifa, F. Izzo, M. Kraković, V. Monetti, A. Langella, Use of surface modified natural zeolite (SMNZ) in pharmaceutical preparations. Part 2. A new approach for a fast functionalization of zeolite-rich carriers, Microporous Mesoporous Mater. 235 (2016) 42–49. https://doi.org/10.1016/j.micromeso.2016.07.043.

[27] P. Cappelletti, A. Colella, A. Langella, M. Mercurio, L. Catalanotti, V. Monetti, B. De Gennaro, Use of surface modified natural zeolite (SMNZ) in pharmaceutical preparations Part 1. Mineralogical and technological characterization of some industrial zeolite-rich rocks, Microporous Mesoporous Mater. 250 (2017) 232–244, https://doi.org/10.1016/j.micromeso.2015.05.048.

[28] E. Kaznowska, J. Depciuch, K. Szmuc, J. Cebulski, Use of FTIR spectroscopy and PCA-LDC analysis to identify cancerous lesions within the human colon, J. Pharm. Biomed. Anal. 134 (2017) 259–268, https://doi.org/10.1016/j.jpba.2016.11.047.

[29] F. Izzo, A. Langella, B. de Gennaro, C. Germinario, C. Grifa, C. Rispoli, M. Mercurio, Chabazite from Campanian Ignimbrite Tuff as a Potential and Sustainable Remediation Agent for the Removal of Emerging Contaminants from Water, Sustainability. 14 (2022) 725, https://doi.org/10.3390/su14020725.

[30] D. Smiljanić, A. Daković, M. Obradović, M. Ožegović, F. Izzo, C. Germinario, B. de Gennaro, Application of Surfactant Modified Natural Zeolites for the Removal of Salicylic Acid—A Contaminant of Emerging Concern, Materials (Basel). 14 (2021) 7728, https://doi.org/10.3390/ma14247728.

[31] G. Della Ventura, R. Vigliaturo, R. Gieré, S. Pollastri, A.F. Gualtieri, G. Iezzi, Infra Red Spectroscopy of the Regulated Asbestos Amphiboles, Minerals 8 (2018) 1–19, https://doi.org/10.3390/min8090413.

[32] M. Ristić, I. Czakó-Nagy, S. Musić, A. Vértes, Spectroscopic characterization of chrysotile asbestos from different regions, J. Mol. Struct. 993 (2011) 120–126, https://doi.org/10.1016/j.molstruc.2010.10.005.

[33] Y. Liu, Z. He, M. Shankle, H. Tewolde, Compositional features of cotton plant biomass fractions characterized by attenuated total reflection Fourier transform infrared spectroscopy, Ind. Crops Prod. 79 (2016) 283–286, https://doi.org/10.1016/j.indcrop.2015.11.022.

[34] M. Defernez, R.H. Wilson, Mid-infrared spectroscopy and chemometrics for determining the type of fruit used in jam, J. Sci. Food Agric. 67 (1995) 461–467, https://doi.org/10.1002/jsfa.2740670407.

[35] R. Briandet, E.K. Kemsley, R.H. Wilson, Discrimination of Arabica and Robusta in instant coffee by Fourier transform infrared spectroscopy and chemometrics, J. Agric. Food Chem. 44 (1996) 170–174, https://doi.org/10.1021/jf950305a.

[36] Y.W. Lai, E.K. Kemsley, R.H. Wilson, Potential of Fourier transform infrared spectroscopy for the authentication of vegetable oils, J. Agric. Food Chem. 42 (1994) 1154–1159, https://doi.org/10.1021/jf00041a020.

[37] A.R. Cotrim, A. Ferraz, A.R. Gonçalves, F.T. Silva, R.E. Bruns, Identifying the origin of lignins and monitoring their structural changes by means of FTIR-PCA and-SIMCA, Bioresour. Technol. 68 (1999) 29–34, https://doi.org/10.1016/S0960-8524(98)00082-0.

[38] J.R. Mansfield, M.G. Sowa, G.B. Scarth, R.L. Somorjai, H.H. Mantsch, Fuzzy C-means clustering and principal component analysis of time series from near-infrared imaging of forearm ischemia, Comput. Med. Imaging Graph. 21 (1997) 299–308, https://doi.org/10.1016/s0895-6111(97)00018-9.

[39] B. Ribeiro da Luz, Attenuated total reflectance spectroscopy of plant leaves: a tool for ecological and botanical studies, New Phytol. 172 (2006) 305–318, https://doi.org/10.1111/j.1469-8137.2006.01823.x.

[40] J.A. Heredia-Guerrero, J.J. Benítez, E. Domínguez, I.S. Bayer, R. Cingolani, A. Athanassiou, A. Heredia, Infrared and Raman spectroscopic features of plant cuticles: a review, Front. Plant Sci. 5 (2014) 305, https://doi.org/10.3389/fpls.2014.00305.

[41] T. Metsalu, J. Vilo, ClustVis: a web tool for visualizing clustering of multivariate data using Principal Component Analysis and heatmap, Nucleic Acids Res. 43 (2015) W566–W570, https://doi.org/10.1093/nar/gkv468.

[42] A. Can, H. Ayvaz, Ç.U. Pala, N. Condelli, F. Galgano, R. Tolve, The potential of near and mid-infrared spectroscopy for rapid quantification of oleuropein, total phenolics, total flavonoids and antioxidant activity in olive tree (Olea europaea) leaves, J. Food Meas. Charact. 12 (2018) 2747–2757, https://doi.org/10.1007/s11694-018-9892-3.

[43] E. Picariello, D. Baldantoni, F. Izzo, A. Langella, F. De Nicola, Soil organic matter stability and microbial community in relation to different plant cover: A focus on forests characterizing Mediterranean area, Appl. Soil Ecol. 162 (2021) 103897.

[44] J.A. Heredia-Guerrero, R. De Lara, E. Domínguez, A. Heredia, J. Benavente, J. J. Benítez, Chemical–physical characterization of isolated plant cuticles subjected to low-dose $γ$-irradiation, Chem. Phys. Lipids. 165 (2012) 803–808, https://doi.org/10.1016/j.chemphyslip.2012.10.003.

[45] G. Liakopoulos, S. Stavrianakou, G. Karabourniotis, Trichome layers versus dehaired lamina of Olea europaea leaves: differences in flavonoid distribution, UV-absorbing capacity, and wax yield, Environ. Exp. Bot. 55 (2006) 294–304, https://doi.org/10.1016/j.envexpbot.2004.11.008.

[46] B.H. Stuart, Infrared Spectroscopy: Fundamentals and Applications, John Wiley & Sons (2005), https://doi.org/10.1002/0470011149.

[47] M. Mercurio, C. Germinario, C. Grifa, F. Izzo, A. Langella, Non-invasive FTIR spectroscopy: New preliminary data for the identification of mineralogical phases forming Cultural Heritage materials, Rend. Online Soc. Geol. Ital. 42 (2017) 115–118. https://doi.org/10.3301/ROL.2017.27.

[48] L. España, J.A. Heredia-Guerrero, P. Segado, J.J. Benítez, A. Heredia, E. Domínguez, Biomechanical properties of the tomato (Solanum lycopersicum) fruit cuticle during development are modulated by changes in the relative amounts of its components, New Phytol. 202 (2014) 790–802, https://doi.org/10.1111/nph.12727.

[49] A. Prigioniero, D. Zuzolo, Ü. Niinemets, A. Postiglione, M. Mercurio, F. Izzo, M. Trifuoggi, M. Toscanesi, P. Scarano, M. Tartaglia, R. Sciarrillo, C. Guarino, Particulate matter and polycyclic aromatic hydrocarbon uptake in relation to leaf surface functional traits in Mediterranean evergreens: Potentials for air phytoremediation, J. Hazard. Mater. 435 (2022), 129029, https://doi.org/10.1016/j.jhazmat.2022.129029.

[50] A. Ladhari, A. Zarrelli, M.C. Di Meo, M. Ghannem, M. Ben Mimoun, Physiological mechanisms and adaptation strategies of Lactuca sativa L. in response to Olea europaea L. and Ficus carica L. allelochemicals, South African J. Bot. 147 (2022) 106–118, https://doi.org/10.1016/j.sajb.2022.01.002.

[51] A. Taamalli, J. Lozano Sánchez, H. Jebabli, N. Trabelsi, L. Abaza, A. Segura Carretero, J. Youl Cho, D. Arráez Román, Monitoring the bioactive compounds status in *Olea europaea* according to collecting period and drying conditions, Energies. 12 (2019) 947, https://doi.org/10.3390/en12050947.

[52] S. Sharma, R. Chophi, R. Singh, Forensic discrimination of menstrual blood and peripheral blood using attenuated total reflectance (ATR)-Fourier transform infrared (FT-IR) spectroscopy and chemometrics, Int. J. Legal Med. 134 (2020) 63–77, https://doi.org/10.1007/s00414-019-02134-w.